




Targeting acetyl-CoA metabolism attenuates the formation of fear memories through reduced activity-dependent histone acetylation

Desi C. Alexander^{a,b,1}, Tanya Corman^{a,1}, Mariel Mendoza^{a,c}, Andrew Glass^d, Tal Belity^e, Ranran Wu^{a,c}, Rianne R. Campbell^f, Joseph Han^f, Ashley A. Keiser^f, Jeffrey Winkler^d, Marcelo A. Wood^f, Thomas Kim^g, Benjamin A. Garcia^{a,c}, Hagit Cohen^{e,h}, Philipp Mews^{i,2}, Gabor Egervari^{a,j,2}, and Shelley L. Berger^{a,b,j,k,2} 

Contributed by Shelley L. Berger; received August 12, 2021; accepted June 26, 2022; reviewed by Ted Abel and Eric Verdin

Histone acetylation is a key component in the consolidation of long-term fear memories. Histone acetylation is fueled by acetyl-coenzyme A (acetyl-CoA), and recently, nuclear-localized metabolic enzymes that produce this metabolite have emerged as direct and local regulators of chromatin. In particular, acetyl-CoA synthetase 2 (ACSS2) mediates histone acetylation in the mouse hippocampus. However, whether ACSS2 regulates long-term fear memory remains to be determined. Here, we show that *Acss2* knockout is well tolerated in mice, yet the *Acss2*-null mouse exhibits reduced acquisition of long-term fear memory. Loss of *Acss2* leads to reductions in both histone acetylation and expression of critical learning and memory-related genes in the dorsal hippocampus, specifically following fear conditioning. Furthermore, systemic administration of blood-brain barrier-permeable *Acss2* inhibitors during the consolidation window reduces fear-memory formation in mice and rats and reduces anxiety in a predator-scent stress paradigm. Our findings suggest that nuclear acetyl-CoA metabolism via ACSS2 plays a critical, previously unappreciated, role in the formation of fear memories.

epigenetics | histone acetylation | fear conditioning | learning and memory | mass spectrometry

Histone acetylation is a major regulator of many types of long-term memory, including fear memories (1). The formation of long-term memories (LTMs) involves the remodeling of synapses between firing cells, requiring robust transcription of plasticity-dependent genes (2). The initial wave of gene expression involves a set of genes called the immediate early genes (IEGs), which are up-regulated within 30 min of neuronal stimulation and which initiate downstream gene expression (3). The transcription of IEGs is facilitated by the deposition of histone acetylation at their promoters, and the subsequent removal of these activating marks results in down-regulation of IEG transcripts (4). Histone acetylation is balanced by the activity of histone acetyltransferases (HATs), such as CREB-binding protein (CBP) and histone deacetylases (HDACs), and this balance is of critical importance in the brain (4).

Because histone acetylation plays a key role in the formation of LTMs, epigenetic proteins have become attractive targets for therapeutic memory manipulation. For example, class I HDAC inhibitors are being actively pursued as enhancers of memory in mouse models of Alzheimer's disease (5). Inhibitors of CBP and/or its homolog p300, which reduce LTM in the dorsal hippocampus (dHPC) and basolateral amygdala, have been proposed as therapeutic agents for the treatment of posttraumatic stress disorder (PTSD) (6). However, CBP is not an ideal target; null mice are embryonic lethal (7). In humans, loss of a single allele of CBP or its paralogue, p300, results in Rubinstein-Taybi syndrome, a condition characterized by severe intellectual disability (7–9).

The substrate for histone acetylation is the central metabolite acetyl-coenzyme A (acetyl-CoA). Although synthesized in the mitochondria as part of central metabolism, acetyl-CoA is also produced throughout the cell, where it serves as a key substrate for the biosynthesis of lipids, ketones, and the neurotransmitter acetylcholine (10), as well as for acetylation of proteins. Several acetyl-CoA-producing enzymes translocate into the nucleus, where they aid in gene expression by producing a pool of acetyl-coA for direct use by HATs (11, 12). In mammalian cells, citrate is harvested from the citric acid (TCA) cycle and converted to acetyl-coA through the enzyme ATP citrate lyase (ACLY). ACLY thus plays a critical role in maintaining histone acetylation in mammals, particularly in highly mitotic (and glycolytic) cancer cells (13). Other metabolic enzymes also support histone acetylation. The pyruvate dehydrogenase complex (PDC) contributes to histone acetylation during early embryonic development, and the mammalian homolog

Significance

Long-term memories associated with traumatic events underlie many mental health issues, including posttraumatic stress disorder, and are difficult to disrupt using existing therapies. Histone acetylation regulates long-term fear-memory formation, which implicates acetyl-coenzyme A (acetyl-CoA)-producing metabolic enzymes in the encoding of fear. Here, we investigate whether ablating acetyl-CoA synthetase 2 (ACSS2), an important source of acetyl-CoA in the brain, can disrupt the formation of fear memories. We show that mice lacking ACSS2, while normal under baseline conditions, show deficits in long-term fear memory. These learning-related deficits are underpinned by training-specific reductions in histone acetylation and gene transcription. Furthermore, systemic administration of small-molecule ACSS2 inhibitors similarly blocks the formation of fear memories, implicating therapeutic relevance for this pathway.

Competing interest statement: S.L.B. and P.M. are cofounders of EpiVario, Inc. T.K. is the chief executive officer of EpiVario. EpiVario provided experimental compounds (ACSS2i) through a sponsored research agreement with the University of Pennsylvania.

Copyright © 2022 the Author(s). Published by PNAS. This article is distributed under [Creative Commons Attribution-NonCommercial-NoDerivatives License 4.0 \(CC BY-NC-ND\)](https://creativecommons.org/licenses/by-nc-nd/4.0/).

¹D.C.A. and T.C. contributed equally to this work.

²To whom correspondence may be addressed. Email: philipp.mews@mssm.edu, egervari@penmedicine.upenn.edu, or bergers@penmedicine.upenn.edu.

This article contains supporting information online at <http://www.pnas.org/lookup/suppl/doi:10.1073/pnas.2114758119/-DCSupplemental>.

Published August 3, 2022.

of ACS2, acetyl-CoA synthetase 2 (ACSS2) is required to maintain histone acetylation during metabolic stress, such as glucose starvation (14). In contrast to PDC or ACLY, which rely on products of glucose metabolism, ACSS2 can recycle acetate released by HDAC reactions (15). This capability for acetate reprocessing implies that ACSS2 may be of particular importance in postmitotic cells like neurons, which do not dilute their nuclear metabolic pools through cell division.

ACSS2 is critical for histone acetylation in the adult mouse brain, particularly during spatial-memory formation (16, 17). However, an important outstanding question is whether ACSS2 is involved in highly durable forms of LTM, such as fear memory. If this were the case, ACSS2 might represent a pharmacological target to ameliorate diseases of persistent stress memory associated with trauma.

In this study, we examined the contribution of ACSS2 to formation of fear memory in rodent models. We utilized two approaches: a null ACSS2 mouse model and pharmacological inhibition of ACSS2 using small-molecule inhibitors. Our results

support a crucial role for ACSS2 in fear memory via regulation of histone acetylation and transcription of key IEGs. Overall, our findings underscore a profound impact of a metabolic protein, ACSS2, on the epigenome and transcriptome in the learning brain and establish ACSS2 as a promising pharmacological target.

Results

Generation of a Constitutive ACSS2^{KO} Mouse. To examine the role of ACSS2 in learning and memory, we used CRISPR/Cas9 to engineer mice with a deletion of exons 3 to 7 of the *Acss2* locus (*Acss2*^{Δ3-7}). We designed guide RNAs to target the Cas9 enzyme to intronic regions upstream of exon 3 and downstream of exon 7. The resulting deletion introduces multiple premature stop codons, with the first located at the new junction between exon 2 and exon 8 (Fig. 1A).

We injected these guides, along with Cas9 mRNA, into fertilized eggs harvested from C57Bl6/J mice. To remove potential mutations derived from off-target Cas9 activity, we crossed

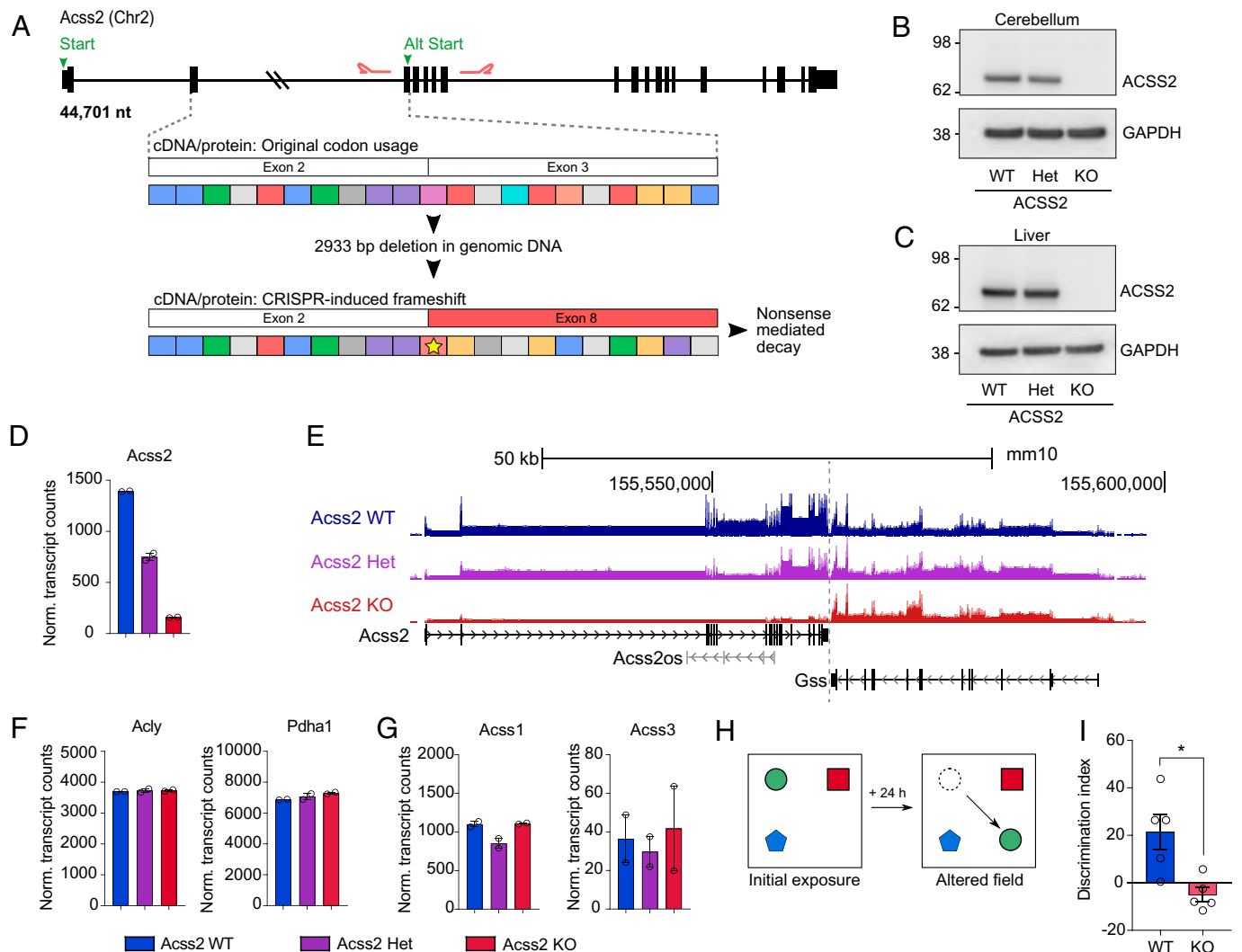


Fig. 1. Generation and characterization of a constitutive *Acss2*^{KO} mouse. (A) Diagram showing CRISPR strategy to KO *Acss2* in mouse. Guide RNAs are shown as red hairpins; stop codons as yellow stars. (B) Representative Western blot of ACSS2 in brain (cerebellum), showing age-matched WT, *Acss2*^{Het}, and *Acss2*^{KO}. (C) Western blot of ACSS2 expression in liver. (D) *Acss2* mRNA levels shown as normalized transcript counts mapped to *Acss2* exons. (E) University of California, Santa Cruz, genome browser tracks showing dose-dependent reduction at the *Acss2* locus (Left) but unchanged neighboring gene (*Gss7*, Right). (F) Bar charts showing messenger RNA (mRNA) expression levels of *Acly* and *Pdha1*, the catalytic subunit of the PDC complex. (G) Bar charts of *Acss1* and *Acss3* mRNA levels. (H) OLM assay showing object positions during training (Left) and recall (Right). (I) Bar graph showing OLM discrimination score for WT and *Acss2*^{KO} mice. WT: *n* = 5; KO: *n* = 5. **P* = 0.011, unpaired *t* test. All data presented as mean ± SEM. cDNA, complementary DNA; Het, heterozygous; Norm., normalized.

founder *Acss2*^{Δ3-7} mice back to the founder C57BL6/J strain for three generations. A previously generated mouse homozygous-null knockout (KO) of ACSS2 was viable (18, 19); however, this strain was unavailable, and its mixed C57BL6/129 background reduced suitability for behavioral research.

Mice harboring biallelic copies of *Acss2*^{Δ3-7} (hereafter called *Acss2*^{KO}) exhibited complete loss of ACSS2 protein across all tissues, including the cerebellum (Fig. 1B) and liver (Fig. 1C). *Acss2* mRNA was ablated across the entire *Acss2* locus, including upstream of the 5' cut site (Fig. 1D–E), likely through nonsense-mediated decay (20). Importantly, the *Acss2*^{KO} line is viable, phenotypically normal under standard housing conditions, shows no premature mortality, and breeds consistently with no reductions in litter size, consistent with the previous ACSS2 null mouse (18, 19). Histologic analysis of the *Acss2*^{KO} brain showed no gross anatomical deficits (SI Appendix, Fig. S1B).

Loss of one enzymatic source of acetyl-CoA can result in compensation from other acetyl-CoA-producing enzymes (13). Acetyl-CoA, as a central metabolite, can be produced by a number of enzymes, including ACLY in the cytosol and PDC in the mitochondria; as mentioned, both enzymes can translocate into the nucleus under certain conditions (13, 21, 22). Within RNA-sequencing (RNA-seq) datasets, we found no increased transcription of *Achy* or any PDC components (including *Pdha1*, which encodes the active site of the E1 subunit) in the dHPC of the *Acss2*^{KO} mice (Fig. 1F and SI Appendix, Fig. S1A), nor up-regulation of other acetyl-coA synthetase family members (namely, *Acsl1* and *Acsl3*) (SI Appendix, Fig. S1G). These results show that loss of *Acss2* is well tolerated in the brain under baseline conditions.

Acss2^{KO} Mice Are Not Behaviorally Impaired under Baseline Conditions. We next tested the mice for mild neurological impairments, using a battery of assays to test locomotion, anxiety, and working memory. The open-field assay simultaneously measures locomotion and anxiety in rodents by quantifying distance traveled and affinity toward the periphery of the testing arena (i.e., thigmotaxis) (SI Appendix, Fig. S1C). Representative traces of both wild-type (WT) and *Acss2*^{KO} mice generated by ANY-maze during this interval were visually similar (SI Appendix, Fig. S1D). We found that *Acss2*^{KO} mice exhibited no difference in path length (SI Appendix, Fig. S1E) or thigmotaxis (SI Appendix, Fig. S1F) compared with WT controls, demonstrating normal locomotion and anxiety.

We then examined working memory, which involves processes upstream of transcription-dependent long-term-memory consolidation (3, using a y-maze test of spontaneous alternation. This assay relies on correct recall of previous paths when choosing a new maze arm to explore (23) (SI Appendix, Fig. S1G). *Acss2*^{KO} mice showed no deficit, engaging in spontaneous alternations at WT-mice levels (SI Appendix, Fig. S1H). Thus, loss of ACSS2 does not impair non-LTM behavior.

Loss of ACSS2 Impairs LTM, Including Fear Memory. We investigated the role of ACSS2 in LTM, first testing the *Acss2*^{KO} mouse for impairments of spatial memory, using an object location memory (OLM) test (3) (Fig. 1H). *Acss2*^{KO} mice exhibited significantly reduced discrimination index compared with WT controls (Fig. 1I), thus indicating poor consolidation of spatial memories.

As a model for more robust LTM with negative emotional valence, we utilized a cued fear-conditioning (FC) paradigm, which pairs an aversive stimulus with contextual and auditory cues (24), and persists for weeks (25). We subjected age-matched

Acss2^{KO} and WT mice to a standard FC paradigm (Fig. 2A), placing mice in an arena for 2 min of exploration, then presenting an auditory cue coincident with a mild foot shock (1 mA, 2s); the mice were returned to the arena 24 h after training to test context and cue (auditory) recall.

The previous results of *Acss2*^{KO} mice maintaining working memory but having poor LTM (Fig. 1 and SI Appendix, Fig. S1), predicted that acquisition of fear memory may be normal in the *Acss2*^{KO} mice but that consolidation of memory may be defective. Analysis of freezing during training showed that *Acss2*^{KO} mice readily responded to FC in the short term and exhibited increased freezing with every presentation of the tone-shock pair (Fig. 2B and SI Appendix, Fig. S3B). However, during recall sessions, *Acss2*^{KO} mice performed significantly worse than WT controls; WT mice responded robustly to the onset of the first tone by increasing freezing 1.68-fold. By contrast, *Acss2*^{KO} mice did not significantly respond to the conditioned stimulus (Fig. 2C and SI Appendix, Fig. S2C). Ruling out auditory deficit in the *Acss2*^{KO} mouse as a potential confounder, we found that the *Acss2*^{KO} mice performed at WT-mice levels in an acoustic startle response assay (Fig. 2E (SI Appendix, Fig. S2H). Importantly, *Acss2*^{KO} mice also froze significantly less often than WT mice during contextual recall (Fig. 2D and SI Appendix, Fig. S2D), which depends on the recall of spatial memories. Together, these results indicate that *Acss2*^{KO} mice are deficient in the consolidation of long-term fear memory.

Acss2^{KO} Mice Exhibit Impairment of Histone Acetylation Relevant to LTM.

Histone acetylation is required for the transcription of activity-dependent genes, and certain histone acetylation sites such as H4K5ac (26), H4K8ac (27), and H3K27ac (28) are linked to activity-related gene expression in learning and memory models. We analyzed histone posttranslational modifications during LTM formation in FC, using “bottom-up” mass spectrometry, which allows unbiased quantification of global histone posttranslational modifications (29). We subjected an age-matched cohort of mice to contextual FC, using a single-shock paradigm (1.5 mA, 2s), which generated long-term fear memories (SI Appendix, Fig. S3E–G) and provided a clearly defined starting point, allowing time-specific sample collection (Fig. 3A). To capture activity-related histone acetylation, we killed mice 30 min after acquisition (Fig. 3A) and analyzed the dHPC, since contextual FC relies on this brain region. Home-cage-housed WT and *Acss2*^{KO} mice served as baseline controls.

In WT mice, we found significant increases in H4K5ac 30 min after FC (Fig. 3B), consistent with previous reports of up-regulation in the dHPC after FC (26). There were no significant differences in histone acetylation between WT and *Acss2*^{KO} mice at baseline (Fig. 3B); in contrast, following FC, *Acss2*^{KO} mice exhibited marked reductions in H3K9ac when compared with WT FC and baseline KO H4K5ac when compared with WT FC. However, not all histone acetylation sites were similarly affected by the loss of ACSS2; for example, H3K18ac and H3K23ac showed no fluctuations upon ACSS2 deletion. We also found no impact on acetylation of histone H2B (SI Appendix, Fig. S3A). These results show that certain histone acetylation sites respond quickly to behavioral stimulation in an *Acss2*-dependent manner.

Acss2^{KO} Mice Exhibit Dampened Transcriptional Response to FC.

Histone acetylation is required for the expression of activity-related genes in learning and memory (7, 30). Given the observed changes in global histone acetylation during FC, we next assayed transcriptional responses in the WT and *Acss2*^{KO}

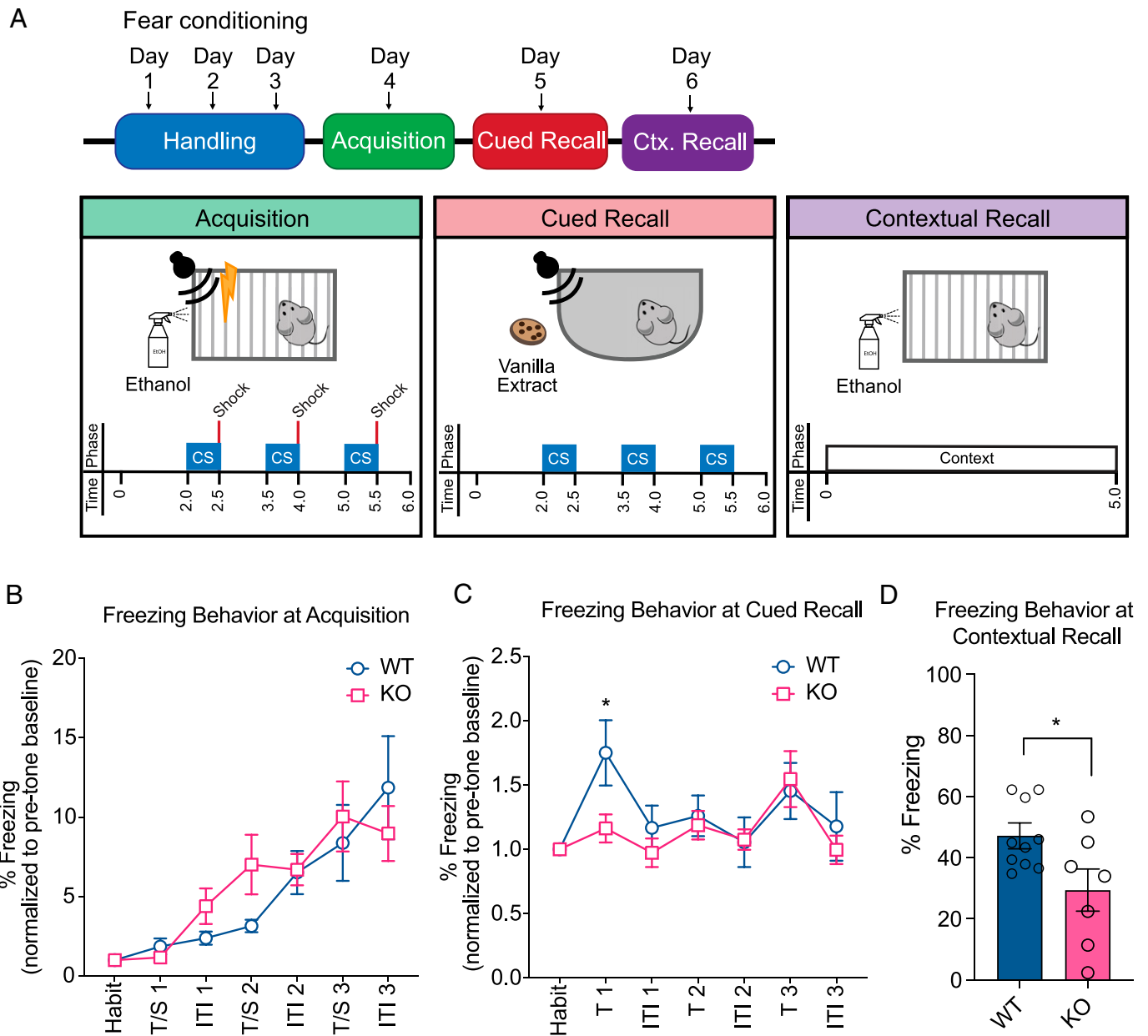


Fig. 2. Loss of *ACSS2* impairs FC. (A) FC schematic, showing training/acquisition (Left), cued/auditory recall (Middle), and contextual (ctx.) recall (Right). (B) Fear response during training/acquisition reflected as fold change over freezing within the pretone interval. Periods binned by period: pretone, intertone interval (ITI), tone (T), or tone-shock pairing (T/S). $P = ns$, 2-way ANOVA. (C) Fear response during cued/auditory recall reflected as fold change over pretone interval. $*P = 0.0208$, 2-way ANOVA, post hoc Fisher's least significant difference. (D) Fear response during contextual recall reflected as percent time freezing, averaged over the entire recall period (5 min). $P = 0.0305$, unpaired t test. Data are presented as mean \pm SEM. Habit., habituated; ns, not significant; CS, conditioned stimulus.

brain. RNA-seq was performed from slices of dHPC reserved from the same mice used to examine histone acetylation. A direct comparison between WT and *Acsc2*^{KO} mice after FC showed acute transcriptional alteration (Fig. 4A), with 3,987 genes significantly differentially expressed between genotypes (adjusted $P [P_{adj}] < 0.05$). Of these, the 2,319 genes that were enriched in WT mice after FC featured gene ontology (GO) categories related to LTM formation, including learning, calcium-ion transport, and transmembrane ion channels (Fig. 4C). Aside from *Acsc2* itself, the most significantly enriched genes in the WT dHPC after FC included genes required for the remodeling of activated synapses, including the ionotropic glutamate (*N*-methyl-D-aspartate [NMDA]) receptor subunit epsilon-2 (*Grin2b*) (31, 32); p35 (*Cdk5r1*), an enhancer of Cdk5-mediated synaptic plasticity (33); and nitric oxide

synthetase 1 (*Nos1*), which generates nitric oxide at the postsynaptic density for use as a second messenger, neurotransmitter, and vasodilator (34). We also noted down-regulation of the histone acetyltransferases CBP, p300, and Kat2a (*Gcn5*) in the KO mouse; all three enzymes have been implicated in learning and memory (32, 34–36) (SI Appendix, Fig. S4E).

Instead of LTM-related genes that increase in the WT mouse following FC, the 1,668 *Acsc2*^{KO}-biased genes showed a distinct focus on pathways downstream of transcription, with top GO terms associated with protein translation (including ribosomal biogenesis and ribosomal RNA processing) (Fig. 4D). The transcriptome of *Acsc2*^{KO} mice also reflects increased metabolic needs of activated neurons, such as enrichment for key genes involved in every stage of the oxidative phosphorylation pathway. However, consistent with previous results (Fig. 1F),

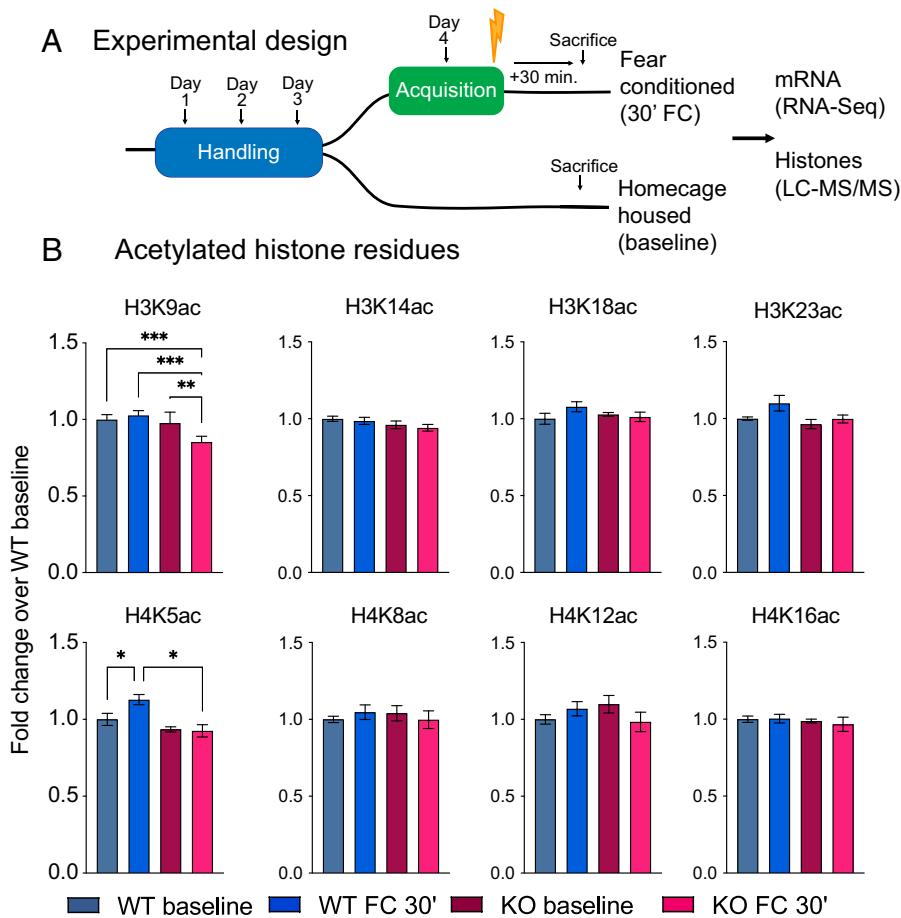


Fig. 3. ACSS2 KO mice exhibit reduced histone acetylation in an activity-dependent context. (A) Schematic of paired histone acetylation and RNA-seq study design. (B) Bar graphs showing histone acetylation levels expressed as fold-change over WT baseline (abundance per average baseline abundance). One-way ANOVA, post hoc Fisher's least significant difference. * $P < 0.05$, ** $P < 0.01$, *** $P < 0.001$. Data are presented as mean \pm SEM. LC-MS/MS, liquid chromatography–tandem mass spectrometry.

no up-regulation was observed in *Acly* or *Pdha1*. In fact, transcription of *Acly* dropped in the *Acss2*^{KO} hippocampus upon FC (SI Appendix, Fig. S4F), agreeing with previous reports of its activity-dependent transcription (37).

Given the number of genes dysregulated in *Acss2*^{KO} after FC, we reasoned that some of the alterations could be constitutive changes in the mutant mouse. Surprisingly, the hippocampal transcriptome of *Acss2*^{KO} mice was remarkably similar to that of WT mice without FC (Fig. 4B); in fact, aside from down-regulation of *Acss2*, only one gene (*Epop*) was significantly up-regulated (Fig. 4B).

To determine how the dHPC transcriptome of WT and *Acss2*^{KO} mice responded to the stress of FC, we compared FC mice of each genotype to baseline controls. WT mice showed robust increase in expression of a subset of IEGs, including *Egr2*, *Egr1*, *Arc*, and *Fos* (SI Appendix, Fig. S4A). The expression of IEGs in WT mice was reflected in a preponderance of GO terms related to DNA-templated gene transcription (SI Appendix, Fig. S4B). In contrast, *Acss2*^{KO} mice up-regulated only six genes, of which three (*Arc*, *Egr2*, and *Fos*) were IEGs (SI Appendix, Fig. S4B).

Plotting the relative expression of 12 well-characterized IEGs, we found that the induction of most was attenuated in *Acss2*^{KO} mice following FC. In all cases, the fold-change between baseline and fear-conditioned *Acss2*^{KO} mice was less than in WT mice (Fig. 4E). A heat map of the top 80 most differentially expressed genes (DEGs) between WT mice before and after FC (by P_{adj}), showed a similar trend, where the expression of highly up-regulated genes was dampened in *Acss2*^{KO} mice (Fig. 4F). We confirmed these results using qRT-PCR analysis of five IEGs (*Fos*, *Nr4a2*, *Fosl2*, *Egr1*, and *Jun*) (SI Appendix, Fig. S4D).

These results indicate that ACSS2 is essential for the expression of most IEGs and suggest that LTM deficits in *Acss2*^{KO} mice are tied to reduced activity-dependent transcription. The contrast between ACSS2's minimal impact on baseline expression and its significant impact on activity-dependent transcription may underlie the equivalent performance of *Acss2*^{KO} mice to WT controls on LTM-independent behaviors (SI Appendix, Fig. S1), and the poor performance of *Acss2*^{KO} on assays requiring LTM (Figs. 1 and 2).

Pharmacological Disruption of ACSS2 Inhibits LTM Formation.

Our characterization of ACSS2^{KO} mice revealed a requirement for ACSS2 in fear-memory consolidation. This finding led us to ask whether pharmacological inhibition of ACSS2 would similarly disrupt fear-memory consolidation, as this could represent a potential therapeutic as a short-acting stress-memory disruptor. We obtained a commercially available small-molecule inhibitor of ACSS2 (cACSS2i) shown to be potent and specific in HepG2 cells (19). Utilizing human preneural NT2 cells, we assessed histone acetylation following treatment with cACSS2i, finding that cACSS2i substantially reduced H3K9ac over a range of concentrations (Fig. 5A).

To address the effect of the inhibitor on brain and behavior, we investigated whether ACSS2i reduces LTM in mouse behavioral models similarly to the genetic disruption of ACSS2. First, we examined the ability of ACSS2i to cross the blood–brain barrier (BBB). Pharmacokinetic assessment in rats revealed that cACSS2i was present in brain homogenate following intravenous (IV) administration of cACSS2i at 5 min, 1 h, and 4 h after administration, and levels dropped more than 100-fold at 4 h (Fig. 5B). Importantly for potential therapeutic usage

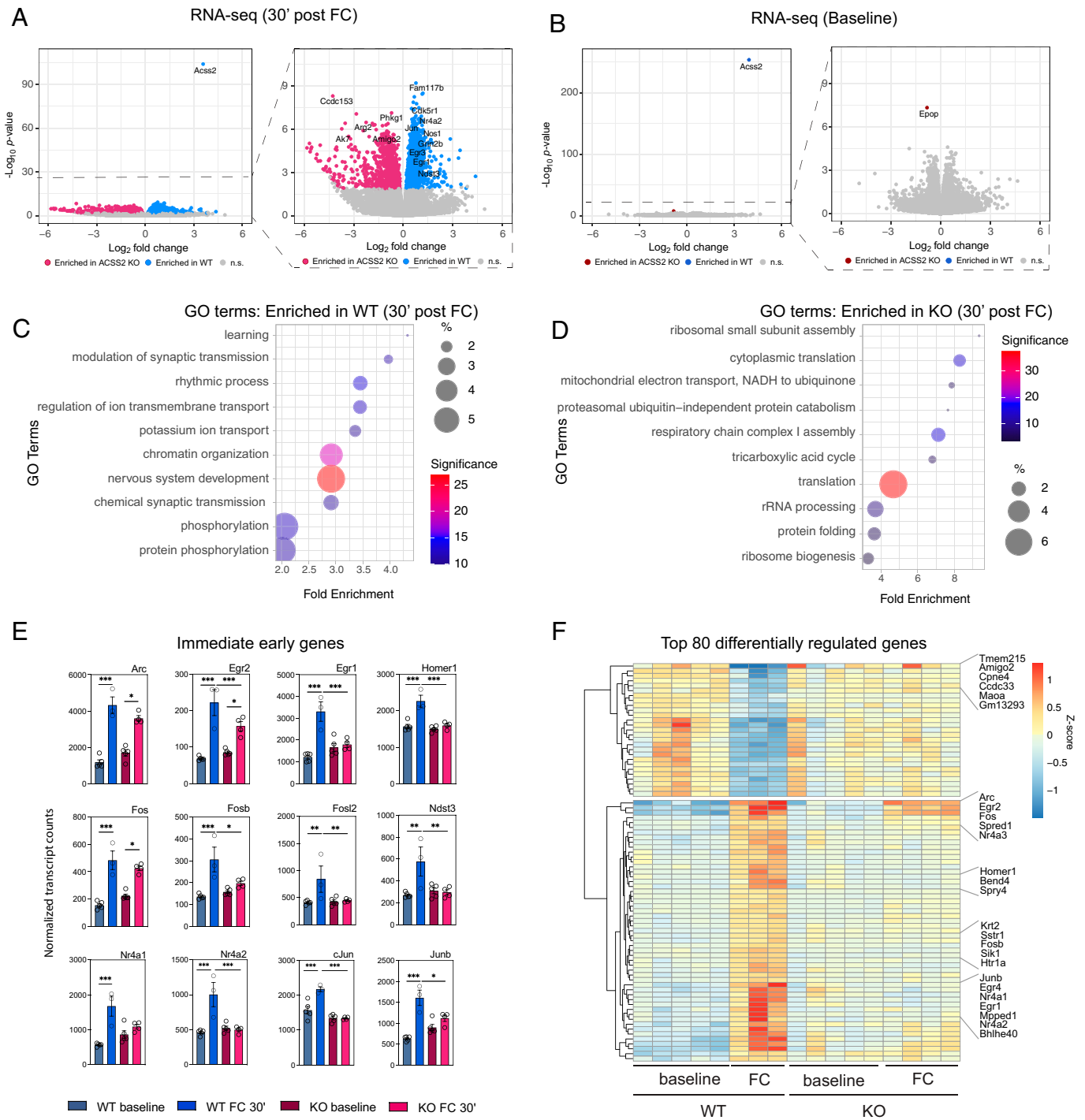


Fig. 4. Loss of ACSS2 negatively impacts the transcription of activity-dependent genes in a FC model. (A) Volcano plot showing gene expression changes between fear-conditioned WT and ACSS2KO mice 30 min after acquisition. Significant genes ($P_{adj} < 0.05$) denoted by colored points. WT FC 30': $n = 5$; KO FC 30': $n = 4$. (B) Volcano plot for gene expression changes between home-cage-housed WT and ACSS2KO mice. WT baseline: $n = 5$; KO baseline: $n = 4$. (C) Top 10 GO terms (Database for Annotation, Visualization and Integrated Discovery [DAVID], biological process [BP]) enriched in WT FC 30' (DAVID, BP) compared with KO FC 30'. (D) Top 10 GO terms enriched in KO FC 30' (DAVID, BP) compared with WT FC 30'. (E) Bar plots of 12 well-characterized IEGs showing normalized transcript counts across all four conditions. WT BL, $n = 5$; WT FC 30', $n = 3$; KO BL, $n = 5$; KO FC 30', $n = 4$. (F) Heat map of top 80 DEGs in WT FC 30' versus baseline (RNA-seq; top 80 genes determined by P_{adj} value). * $P < 0.05$, ** $P < 0.01$, *** $P < 0.001$. Data are presented as mean \pm SEM. ns, not significant; rRNA, ribosomal RNA.

in which a temporally limited effect would be desired, cACSS2i was no longer detected in the brain at 8 h after IV administration, with minimal cACSS2i detected in plasma 24 h following IV administration (SI Appendix, Fig. S5A). In addition, we observed similar kinetics for cACSS2i in mouse hippocampus following administration by intraperitoneal (IP) injection (Fig. 5C).

The cACSS2i was tested on basal locomotor activity via a 30-min open-field assay. Mice injected with cACSS2i displayed equivalent locomotor activity to those injected with dimethyl sulfoxide (DMSO) vehicle, indicating no deleterious effect on movement (Fig. 5D). We tested whether cACSS2i reduces OLM, as described for the $Acsc2^{KO}$. To ensure that the drug remained onboard during the consolidation window,

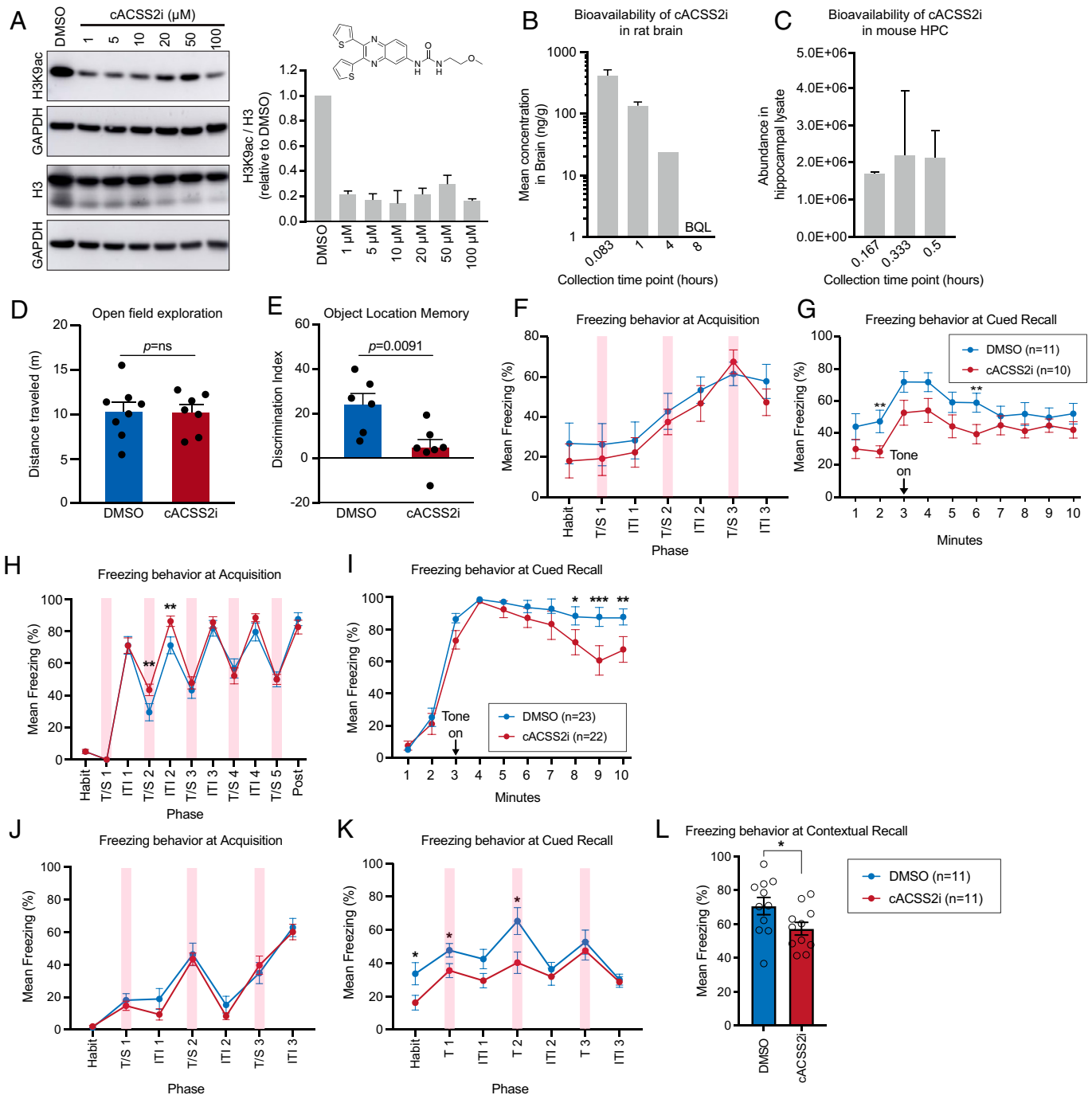


Fig. 5. Small-molecule inhibitor of ACSS2 reduces histone acetylation in vitro, is bioavailable in rodents, and disrupts LTM formation in vivo. (A) Western blot on NT2 cell lysates for H3K9ac, H3, and GAPDH loading following treatment with cACSS2i. Quantification (Right; $n = 2$) shows a reduction in H3K9ac/H3 ratio (one-way ANOVA $F_{6,7} = 30.9$, $P = 0.0001$, post hoc Dunnett test comparing each concentration with DMSO $P_{\text{adj}} \leq 0.0002$). (B) Pharmacokinetic analysis of cACSS2i following IV administration in rat brain homogenate ($n = 3$ animals at time [t] 0.083 and t1; $n = 1$ at t4). cACSS2i is not detected (ND) at 8 h. (C) cACSS2i in mouse hippocampal lysate up to 30 min following IP injection ($n = 2$ for each time point). (D) Open-field assessment in mouse indicates no difference in basal locomotion following IP injection of DMSO or cACSS2i (DMSO, $n = 8$; cACSS2i, $n = 7$). (E) Long-term memory formation is disrupted in cACSS2i-injected animals in the OLM assay (DMSO, $n = 6$; cACSS2i, $n = 7$; $P = 0.0091$, unpaired Student's t test). (F) Freezing behavior in mouse during acquisition with cACSS2i treatment reflected as %time freezing/total time. Freezing during habituation period was averaged; the remaining time was binned into 30-s intervals. Timing of CS-US pairings indicated by transparent red bars. $P = ns$, two-way ANOVA. (G) Freezing behavior during cued recall in mice treated with cACSS2i or DMSO at acquisition plotted as %time freezing/total time, binned into 30-s intervals. Onset of tone marked by black arrow. Significant time points are observed at the onset of cue. Two-way ANOVA, Fisher's LSD, $**P = 0.0308$, $***P = 0.0319$. (H) Freezing behavior in rats during acquisition with cACSS2i plotted as % time freezing/total time. Freezing during habituation period was averaged, remaining time binned into 30-s intervals. Time of CS-US pairings indicated by transparent red bars. Two-way ANOVA, Fisher's LSD, $**P = 0.0375$, 0.0208 . (I) Freezing behavior during cued recall in rats treated with cACSS2i or DMSO at acquisition plotted as %time freezing/total time, binned into 30-s intervals. Onset of tone is marked by a black arrow. Significant time points are observed late in cue presentation. Two-way ANOVA, Fisher's LSD, $*P = 0.0285$, $***P = 0.0003$, $*P = 0.0070$. (J) Freezing behavior in mouse during acquisition with cACSS2i treatment reflected as % time freezing/total time. Freezing during habituation period was averaged, remaining time was binned into 30-s intervals. Timing of CS-US pairings is indicated by transparent red bars. $P = ns$, two-way ANOVA. (K) Freezing behavior during cued recall in mice treated with cACSS2i or DMSO at acquisition plotted as %time freezing/total time, binned into 30-s intervals. Timing of CS indicated by transparent red bars. Two-way ANOVA, Fisher's LSD, $*P < 0.05$. (L) Fear response during contextual recall reflected as %time freezing, averaged over the entire recall period (5 min). $P = 0.0305$, unpaired t test. Data presented as mean \pm SEM. Habit, habituated; CS, conditioned stimulus; US, unconditioned stimulus; ITI, intertone interval; T/S, tone-shock pairing; ns, not significant.

we administered cACSS2i or vehicle by IP injection prior to and immediately following training sessions. During the training sessions, cACSS2i-injected mice explored objects at similar levels to DMSO-injected controls (*SI Appendix, Fig. S5C*).

OLM was assessed 24 h later with one object moved to a different location. During recall, vehicle-injected mice exhibited increased exploration of the object moved to a novel location (Fig. 5*E*), while, in contrast, mice injected with cACSS2i displayed a reduced discrimination index relative to the control counterparts (Fig. 5*E*). We also noted a slight increase in exploration in cACSS2i-injected animals during recall, consistent with reduced memory of the arena (*SI Appendix, Fig. S5D*). Thus, cACSS2i administration reduces LTM in OLM similar to genetic mutations of ACSS2, serving as proof of concept that pharmacological inhibition of ACSS2 is capable of disrupting memory consolidation.

ACSS2 Inhibition Reduces Fear Memory in a Rodent Cued-FC Model. We next investigated the ability of ACSS2i to disrupt fear-memory consolidation in a rodent cued-FC model, as discussed above and schematized in Fig. 2*A* and *SI Appendix, Fig. S6A*. In two separate experiments, we administered cACSS2i via IP injection prior to and immediately following fear training. At 24 h postconditioning, mice were placed in an altered context and subjected to either a singular extended tone or a three-tone sequence in the absence of the foot shock. While DMSO-injected and cACSS2i-injected mice exhibited similar behavior during FC acquisition (Fig. 5*F* and *J*), there was reduced freezing by cACSS2i mice during cued recall, as well as a general reduction of freezing during the pre-tone period (Fig. 5*G* and *K*). Administration of cACSS2i similarly reduced contextual recall (Fig. 5*L*). These results recapitulated those initially observed in the ACSS2^{KO} model. However, the effect on histone acetylation was apparently small, because we did not detect reduction of H3K9ac via mass spectrometry (*SI Appendix, Fig. S5E*).

To test whether administration of cACSS2i outside the consolidation window impacts future encoding of fear memory, we performed two additional experiments. First, we modified the above FC paradigm by injecting inhibitor 24 h prior to acquisition (*SI Appendix, Fig. S6C*). We found that this pretreatment did not reduce acquisition, cued recall, or contextual recall (*SI Appendix, Fig. S6D–F*). Second, we injected cACSS2i 24 h after acquisition and 24 h before recall, using a separate injection room to avoid triggering recall of the FC trace (*SI Appendix, Fig. S6G*). Subsequent testing of contextual recall showed no impact of cACSS2i (*SI Appendix, Fig. S6H and I*). These results are consistent with the short half-life in brain of the cACSS2i (Fig. 5*B* and *C*), which, taken together, are attributes that are appropriate for potential utility as a therapeutic.

We then tested fear memory in rats to increase our study rigor through tested cross-species comparison. We examined whether cACSS2i could disrupt fear-memory consolidation in a rat cued-FC assay (*SI Appendix, Fig. S6B*), similar to the mouse experiment above. After a habituation period, rats were exposed to the pairing of an auditory tone coterminating with a mild foot shock. The pairing was repeated for a total of five presentations. We administered cACSS2i via IP injection prior to and immediately following fear training. At 24 h postconditioning, rats were placed in an altered context and subjected to a singular extended tone in the absence of the foot shock. While cACSS2i-injected rats exhibited slightly more freezing at fear acquisition (Fig. 5*H*), we observed reduced freezing in cACSS2i-injected rats during cued recall (Fig. 5*I*).

Overall, these data in mouse and rat indicate that administration of cACSS2i during the consolidation window reduces cued and contextual FC, but that administration outside this window does not impact the establishment of future fear memories, nor does it impair the integrity of those previously encoded.

ACSS2i Injection Results in Reduced Generalized Anxiety and Cued Recall in a Rodent Model of PTSD. To further elucidate the potential of ACSS2 inhibition as a therapeutic for PTSD, we utilized the predator-scent stress (PSS) model, which more thoroughly analyzes levels of specific and generalized anxiety following an aversive event (38, 39). Briefly, rats were exposed to a predator scent or to a sham control with cACSS2i or DMSO vehicle administered through IP injections prior to and following exposure (Fig. 6*A*). Seven days later, generalized anxiety was assessed following PSS exposure with acoustic startle response and elevated plus maze (EPM) assays. In controls, we observed a strong increase in startle amplitude in PSS-exposed animals relative to sham PSS (Fig. 6*B*). Startle amplitude was lower in cACSS2i-injected animals exposed to PSS (Fig. 6*B*). PSS exposure also resulted in a significant increase in Anxiety Index in EPM activity, a metric integrating time spent in open arms of a maze, number of entries to open arms, and total exploration of the maze (Fig. 6*C* and *SI Appendix, Fig. S7*). Strikingly, this increase was blunted in cACSS2i-injected PSS rats relative to DMSO-injected animals (Fig. 6*C*). Importantly, all cohorts displayed similar levels of activity in EPM, indicating that the observed differences were due to variance in anxiety level rather than a disruption of locomotor activity (Fig. 6*D*). Taken together, EPM and acoustic startle response data indicate that cACSS2i administration reduces fear and generalized anxiety behavior in rat models following exposure to PSS.

One day following the testing of anxiety behavior (day 8), rats were re-exposed to the cat litter stimulus in a similar environment and freezing behavior was measured. PSS-exposed, DMSO-injected rats exhibited significant increase in freezing during the reminder session compared with sham-PSS, DMSO-injected animals. In contrast, cACSS2i-injected PSS rats exhibited significantly less freezing than DMSO-injected PSS animals (Fig. 6*E*), on par with sham-PSS-treated rats, indicating reduced fear memory. Finally, we assessed long-term retention of the stress memory in a second recall session 7 d following the first reminder session (day 15). PSS-exposed rats injected with DMSO continued to display significant freezing relative to sham-PSS controls. Again, cACSS2i-injected, PSS-exposed rats displayed decreased freezing (Fig. 6*F*), indicating that reduction in fear memory persisted in cACSS2i-injected, PSS-exposed rats. These results thus suggest that inhibition of ACSS2 disrupts LTM consolidation surrounding trauma exposure.

Development of a newly-synthesized inhibitor of ACSS2. These findings with cACSS2i led us to design and synthesize analogs of ACSS2i in an effort to further improve the window of brain bioavailability and to optimize pharmacokinetics for acute and limited disruption of memory formation. Toward that end, we replaced the methoxyethyl moiety present in ACSS2i with an *n*-pentyl group to generate nACSS2i, with increased lipophilicity and, therefore, increased BBB penetration (40). The newly-synthesized analog was prepared from the isocyanate (triphosgene, Hünig's base, dichloromethane) derived from 2,3-di(thiophen-2-yl)quinoxalin-6-amine (41). This compound (hereafter called nACSS2i) was tested in histone acetylation *in vitro*, and as with the cACSS2i, we observed significant reduction in levels of H3K9 acetylation following treatment with nACSS2i (Fig. 7*A*). Furthermore, we detected nACSS2i

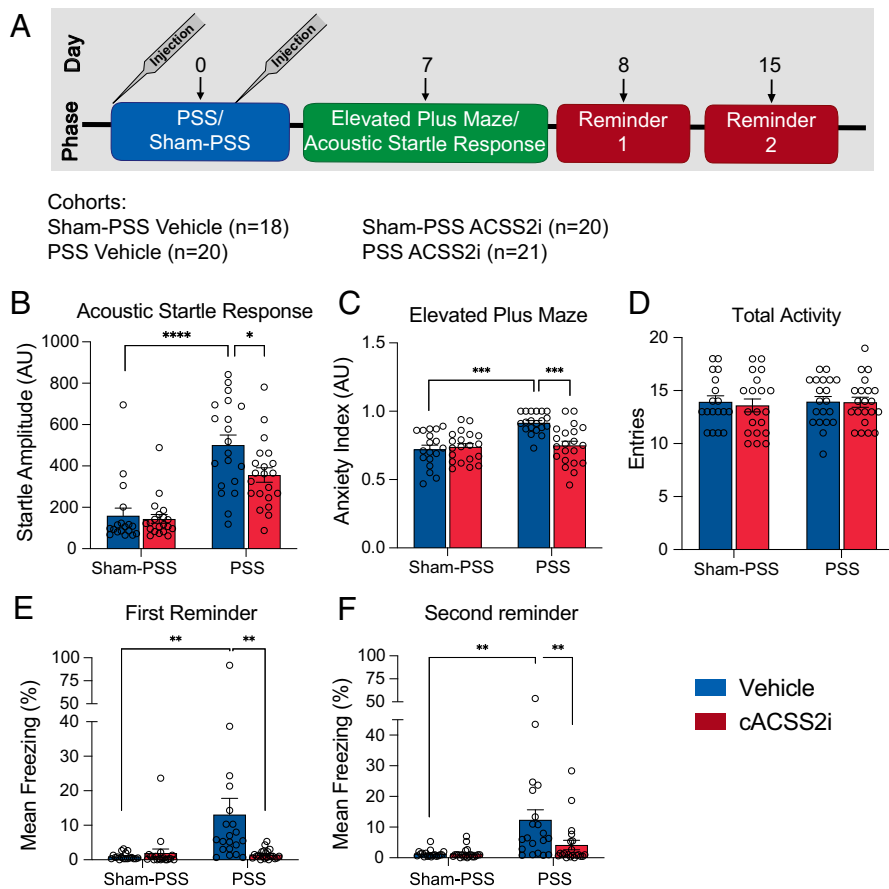


Fig. 6. cACSS2i treatment impairs PSS-induced fear-memory consolidation in rats. (A) Outline of the PSS assay. Rats are exposed to PSS (soiled cat litter) or sham-PSS (fresh cat litter) after they were injected with cACSS2i or DMSO. One week later, anxiety level in animals is measured through EPM and acoustic startle response. The following day, animals are re-exposed to the cat litter stimulus and freezing behavior is measured. A second reminder exposure takes place 1 wk later. (B) PSS-exposed, DMSO-injected rats display increased startle amplitude relative to sham-exposed DMSO-injected rats. cACSS2i-treated, PSS-exposed rats exhibit a reduced startle amplitude. (C) PSS-exposed, DMSO-injected rats have an increased Anxiety Index relative to sham-exposed DMSO-injected rats. cACSS2i-treated, PSS-exposed rats have a lower Anxiety Index. (D) Total entries into open and closed arms of the EPM apparatus to indicate total activity in the assay. No differences between treatment groups were detected. (E) PSS-exposed, DMSO-injected rats display increased freezing relative to sham-exposed DMSO-injected rats upon first reminder. No increase observed in cACSS2i-treated, PSS-exposed rats. (F) Effects observed at first reminder persist 1 wk later at a second reminder session. PSS-exposed, DMSO-injected rats display increased freezing relative to sham-exposed, cACSS2i-treated, PSS-exposed rats. Two-way ANOVA followed by Tukey's multiple comparisons test. * $P < 0.05$, ** $P < 0.01$, *** $P < 0.001$. Data presented as mean \pm SEM. AU, arbitrary units.

in rat plasma and in brain homogenate following IV administration (Fig. 7B and *SI Appendix*, Fig. S5B). Intriguingly, nACSS2i may be cleared faster from the brain than cACSS2i, as nACSS2i was not detected at 4 h after administration (Fig. 7B) and, thus, has potential superior pharmacologic properties aimed at a short therapeutic-treatment window.

To examine whether nACSS2i was similarly able to disrupt fear-memory consolidation, mice were subjected to cued FC, as

described above. While DMSO-injected and nACSS2i-injected mice exhibited equivalent behavior during acquisition (Fig. 7C), we observed reduced freezing in nACSS2i mice during cued recall. This reduction in freezing behavior occurred later in the onset of the tone relative to the phenotype observed with cACSS2i treatment (Fig. 7D). Thus, pharmacological inhibition of ACSS2 with this small molecule may represent a promising therapeutic for PTSD.

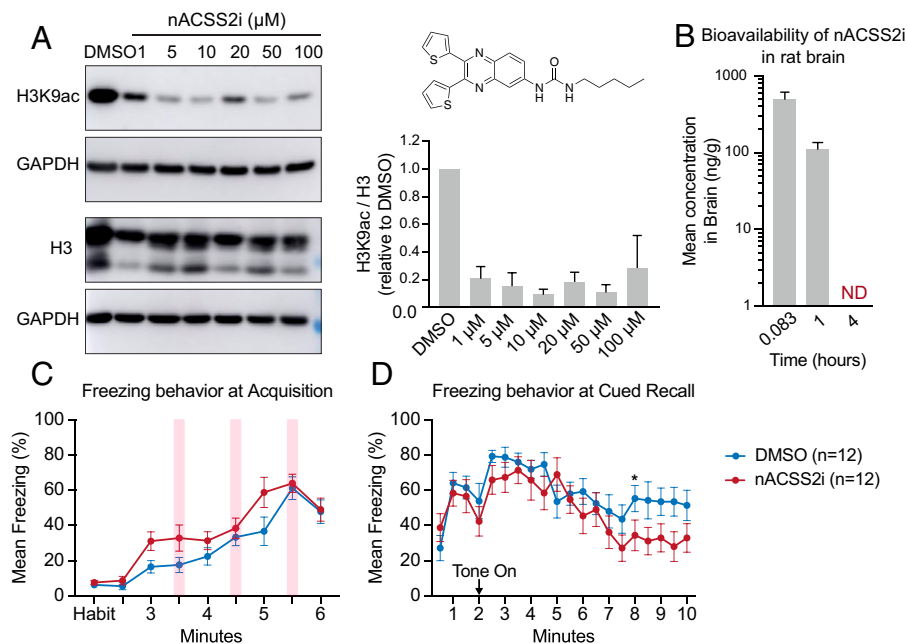


Fig. 7. A small-molecule inhibitor of ACSS2 reduces histone acetylation in vitro, is bioavailable in rodents, and disrupts LTM formation in vivo. (A) Western blot on NT2 cell lysates for H3K9ac, H3, and GAPDH following treatment with nACSS2i. Quantification (Right; $n = 2$) shows a reduction in H3K9ac/H3 (one-way ANOVA $F_{(6, 7)} = 17.38$, $P = 0.0007$; post hoc Dunnett each concentration compared with DMSO, $P_{\text{adj}} \leq 0.0013$). (B) Pharmacokinetic analysis of nACSS2i following IV administration in rat brain homogenate ($n = 3$). (C) Mouse freezing behavior during acquisition with nACSS2i treatment reflected as %time freezing/total time. Freezing during habituation period was averaged; the remaining time was binned into 30-s intervals. Time of CS-US pairings indicated by transparent red bars. $P = \text{ns}$, two-way ANOVA. (D) Freezing behavior during cued recall in mice treated with nACSS2i or DMSO at acquisition plotted as % time freezing/total time, binned into 30-s intervals. Tone onset indicated by black arrow. Significant time points observed late in cue presentation. Two-way ANOVA, Fisher's LSD, ** $P = 0.0408$. Habit, habituated; CS, conditioned stimulus, US, unconditioned stimulus.

Discussion

This study demonstrates that ACSS2 is a critical regulator of fear-memory formation in mice and in rats. Both genetic ablation and small-molecule inhibition of ACSS2 were sufficient to attenuate the consolidation of long-term fear memories. Crucially for therapeutic use, loss of ACSS2 is well tolerated. Mice harboring a whole-body KO of *Acss2* were indistinguishable from WT mice in working memory tests and other LTM-independent behaviors. Histone analyses of mice undergoing active consolidation of fear memories showed significant decreases in the histone marks H4K5ac and H3K9ac in the *Acss2*^{KO} dHPC. Further emphasizing the role of ACSS2 in LTM, this loss of histone acetylation was specific to the fear-conditioned state, as untrained home-cage-housed WT and *Acss2*^{KO} mice had similar levels of acetylation. Similarly, RNA-seq analysis underscored the requirement for *Acss2* during fear-memory consolidation: at baseline, we observed only three DEGs in the dHPC; 30 min after stimulation, this number increased to 3,987 DEGs. Consistent with these results, we found that administering ACSS2i, specifically during fear-memory consolidation, attenuated the persistence of fear memory in both mice and rats. Together, these approaches show that ACSS2 is specifically involved in LTM and point to ACSS2 as a therapeutic target for treating pathological fear memories.

Our results are consistent with previous findings that histone acetylation is a critical regulator of fear-memory formation in the dHPC. Many histone residues are acetylated upon FC, including H3K9ac, H3K14ac, H4K5ac, H4K8ac, and H4K12ac (37). Reductions of the HATs CBP, p300, and *Kat2a* in the dHPC or the amygdala negatively impact the formation of cued and contextual FC (30, 35, 36, 42, 43), as does the inhibition of another HAT (PCAF/*Kat2b*) in the prelimbic cortex (44). Conversely, both cued and contextual FC are strengthened by the ablation of the HDACs HDAC2 and *Sirt1* (45, 46). However, it must be noted that establishing a causal link between activity-dependent histone acetylation and transcription at specific loci has been challenging in the brain (47). Direct manipulation of the epigenome at specific regulatory elements has been shown to tune transcription at the *Fos*, *Npas4*, and *Nr4a1* loci (48, 49), but such causality has yet to be established for other activity-dependent genes (48).

Systemic administration of chemical inhibitors of CBP (6) and HDACs (1, 43, 73, 50–52), respectively, reduce or enhance fear memories when administered during consolidation. Our results show that both *Acss2* genetic ablation by germline KO and ACSS2 inhibition by a small-molecule inhibitor reduced fear memory and histone acetylation similarly to CBP inhibition. Importantly, while genetic KO of CBP or its paralogue, p300, causes embryonic inviability (53, 54), the *Acss2*^{KO} is well tolerated.

We found that reductions of H3K9ac and H4K5ac during FC coincided with the down-regulation of many genes essential for LTM formation. In particular, we found that expression of key IEGs (including *Egr1*, *Nr4a1*, and *Fosb*) was attenuated in fear-conditioned *Acss2*^{KO} mice compared with WT controls. This is consistent with the contribution of CBP to the expression of many IEGs, including *Fos* (30), *Fosb* (55), *Junb*, and *Nr4a1* (56). The findings are also consistent with observations that HDACs, especially HDAC2 and HDAC3, play critical roles in the regulation of *Egr1*, *Fos* (45), *Arc*, and *Nr4a1* (57).

The observed decrease of histone acetylation in the dHPC of fear-conditioned ACSS2^{KO} mice is likely due to reduced acetyl-CoA availability. However, RNA-seq analysis revealed that loss

of *Acss2* also reduces the expression of key HATs, including CBP, p300, and *Kat2a/Gcn5* (*SI Appendix, Fig. S4E*), suggesting a feed-forward loop caused by *Acss2*^{KO}. The histone targets of these HATs include both of the most severely affected residues, H3K9ac and H4K5ac. H3K9ac is deposited mainly by *Gcn5* (58), and H4K5ac by multiple HATs, including CBP/p300 (59). In turn, CBP and p300 are regulated by the IEG *EGR1* (60), which is severely attenuated in the *Acss2*^{KO} mouse after FC, suggesting that the dysregulation of epigenetic enzymes could, in part, be a downstream consequence of *Acss2* manipulation, further affecting histone acetylation. Of note, these interconnected gene regulatory networks underlying LTM formation necessitated examining *Acss2* at the earliest stages of LTM consolidation, that is, beyond the effect on expression of IEGs, it becomes difficult to determine which activity-dependent changes can be tied directly to ACSS2 and which are simply a function of reduced IEG expression.

Also arguing for the specific effects of ACSS2 on LTM, we found that constitutive loss of *Acss2* did not impact global histone acetylation levels in the dHPC. By histone mass spectrometry, we observed no difference between home-caged-housed *Acss2*^{KO} mice and WT controls (Fig. 3). In *Saccharomyces cerevisiae*, by contrast, loss of the *Acss2* homolog *Acs2* results in global histone deacetylation and transcriptional repression (61). This reflects the importance of acetate in yeast metabolism; in the mammalian brain, glucose is the most important bioenergetic substrate. Therefore, in *Acss2*^{KO} mice, the existing histone acetylation present at baseline is likely provided by *ACLY*, which converts glucose-derived citrate into acetyl-CoA, and is known to play an essential role in histone acetylation (13). Though levels of *Acly* did not increase in compensation for *Acss2* loss, the baseline RNA expression level of *Acly* is twice that of *Acss2* in mouse hippocampus (compare Fig. 1 *F* and *G*). Importantly, the striking differences seen in histone acetylation and transcription after neuronal stimulation point to a unique role for ACSS2 during periods of extreme metabolic requirement, like neuronal stimulation (62), a process for which *ACLY* does not appear to compensate.

Indeed, our recent findings investigating the mechanism of chromatin-associated ACSS2 demonstrated that it mediates the transfer of acetate between globally abundant “reservoir” acetylation marks (e.g., K23ac) to lowly abundant “activating” sites (e.g., H3K9ac and H3K27ac) (15). In *S. cerevisiae*, this ACSS2-dependent mobilization of acetyl groups from reservoir sites to activating sites is critical for the expression of genes during early quiescence exit (63). As IEG expression during learning and memory is similarly rapid, this mechanism may explain our observation that only the activating marks H3K9ac and H4K5ac are significantly reduced in the fear-conditioned *Acss2*^{KO} mouse, while reservoir sites like H3K14ac and H3K23ac remain unchanged (Fig. 3).

Our results indicate that the effects of cACSS2i are limited to the labile phase of memory formation (*SI Appendix, Fig. S6 D–I*). While we examined these effects during consolidation, memory recall induces similar molecular and transcriptional processes, called reconsolidation (64). Here, a recalled memory returns to a labile state; blocking translation (65), transcription (66), or histone acetylation (6, 67) during the reconsolidation window weakens the memory trace. Thus, administration of ACSS2i during a clinically induced reconsolidation event could provide specificity toward the pathological memory.

To ensure the viability of ACSS2 to treat memory-related disorders, we focused on improving the ability of ACSS2i to cross the BBB. Our *in vivo* pharmacokinetic data demonstrated that the cACSS2i is able to cross the BBB, and we developed

an ACSS2i (namely, nACSS2i) with altered lipophilicity (40). Furthermore, our medicinal chemistry focused on temporally limited compounds with short half-life and rapid metabolism, which would interfere with LTM consolidation in a therapeutically relevant, sensitive time window. Indeed, cACSSi does not affect “pre-memory” or “post-memory” outside of the treatment window, indicating transient nature of our ACSS2 inhibitor will reduce potential off-target effects associated with the use of a memory-disrupting drug.

We also demonstrated that ACSS2 inhibitors reduce anxiety in a PSS model, which recapitulates heightened anxiety levels and trigger-induced episodes present in PTSD (38). After presentation of an aversive predator scent, rats injected with ACSS2i during the consolidation window not only exhibited reduced freezing in response to predator scent-specific reminders but also showed reduced anxiety in acoustic startle and EPM assays. This reduction of anxiety is also evident in the reduction of pre-tone freezing seen in the contextual FC assay in mice (Fig. 5 G and K). The ability of ACSS2i to disrupt fear-memory consolidation and associated anxiety (Fig. 6) again highlights desirable properties of this small-molecule inhibitor. Thus, taken together, the specificity of ACSS2 toward rapid activity-dependent histone acetylation and gene transcription in the context of LTM formation, while not affecting general health and baseline behavior, makes it an attractive therapeutic target in the treatment of diseases of unwanted memory, including PTSD.

Materials and Methods

A full description of materials and methods is available in *SI Appendix*.

Generation of *Acscs2* KO Mice Using CRISPR-Cas9. We used CRISPR/Cas9 technology to generate constitutive *Acscs2*^{KO} mice as previously described (68). Pairs of single-guide RNAs (sgRNA) targeting intronic regions of the *Acscs2* locus upstream of exon 3 and downstream of exon 7 were designed with the CRISPOR online tool (69) (crispor.org) using the mm10 genome assembly as template. The resulting guides (5′[exon 3]) were selected to maximize specificity while retaining high on-target efficiency. sgRNAs were synthesized by in vitro transcription (T7 High Yield RNA Synthesis Kit; NEB, E2040S). Cas9 mRNA (100 ng/μL; Trilink, L-6125) and both sgRNAs (100 ng/μL each) were diluted in injection buffer (10 mM Tris, pH 7.5; 0.1 mM EDTA). This mix was injected into the cytoplasm of single-cell C57Bl6/J mouse embryos. Resulting founder mice were screened for the desired deletion using primer pairs amplified across each cut site. Sanger sequencing confirmed sites of nonhomologous end joining. To reduce off-target effects, founder mice were backcrossed to C57Bl6/J mice (Jackson Laboratories) for three generations.

General Synthesis of ACSS2 Inhibitors. We dissolved 2,3-di(thiophen-2-yl) quinoxalin-6-amine in anhydrous dichloromethane, and Hünig's base was added. A solution of triphosgene in dichloromethane was added and stirred for 4 h at 25 °C. The corresponding amine was added and stirred for 16 h at 25 °C. The reaction was then concentrated and purified by silica gel chromatography to afford the inhibitor analogs.

1. J. M. Levenson *et al.*, Regulation of histone acetylation during memory formation in the hippocampus. *J. Biol. Chem.* **279**, 40545–40559 (2004).
2. E. R. Kandel, Y. Dudai, M. R. Mayford, The molecular and systems biology of memory. *Cell* **157**, 163–186 (2014).
3. S. G. Poplawski *et al.*, Object-location training elicits an overlapping but temporally distinct transcriptional profile from contextual fear conditioning. *Neurobiol. Learn. Mem.* **116**, 90–95 (2014).
4. K. M. Lattal, M. A. Wood, Epigenetics and persistent memory: Implications for reconsolidation and silent extinction beyond the zero. *Nat. Neurosci.* **16**, 124–129 (2013).
5. J. Gräff, L. H. Tsai, The potential of HDAC inhibitors as cognitive enhancers. *Annu. Rev. Pharmacol. Toxicol.* **53**, 311–330 (2013).
6. S. A. Maddox, C. S. Watts, G. E. Schafe, p300/CBP histone acetyltransferase activity is required for newly acquired and reactivated fear memories in the lateral amygdala. *Learn. Mem.* **20**, 109–119 (2013).
7. E. Korzus, M. G. Rosenfeld, M. Mayford, CBP histone acetyltransferase activity is a critical component of memory consolidation. *Neuron* **42**, 961–972 (2004).

Acscs2i Administration. *Acscs2i* inhibitors were dissolved in 30% (weight per volume) 2-hydroxypropyl-β-cyclodextrin and 1 to 5% DMSO. For the test results shown in Fig. 5 D–G, 100 mM acetate was included as a buffer. The 4 mg/kg doses were IP injected.

Quantification and Statistical Analysis. Sample sizes, test statistics, degrees of freedom, and *P* values are noted throughout in the main text and figure legends. For FC assays, no genetic KO mice were excluded. Otherwise, animals were excluded for unsuccessful IP injections. For OLM, mice were excluded if the total object exploration was <10 s. All statistics were performed using Prism 9 (GraphPad Software). Univariate analysis of variance (one-way ANOVA) was performed for histone acetylation and qRT-PCR data. Repeated-measure ANOVA determined differences in cued FC. A two-way ANOVA was performed in behavioral assays with two treatment groups assayed over multiple conditions (PSS, OLM exploration). Significant differences were followed by Fisher's least significant difference test when appropriate. Pairwise comparisons were made using Student's *t* test after testing for normality and equal variance. The threshold for statistical significance was considered $\alpha = 0.05$ for all experiments.

Data Availability. RNA-sequencing and mass spectrometry data have been deposited in the National Center for Biotechnology Information Gene Expression Omnibus repository under accession no. [GSE199887](https://www.ncbi.nlm.nih.gov/geo/query/acc.cgi?acc=GSE199887) (RNA-Seq) (70) and with Chorus (no. [1745](https://www.chorusdb.org/entry/1745)) (MS) (71).

ACKNOWLEDGMENTS. We thank E. Korb and K. Wellen for insightful discussions on behavior and metabolism, respectively. *Acscs2*^{KO} were generated with the University of Pennsylvania Transgenic and Chimeric Mouse Core (Institute for Diabetes, Obesity and Metabolism, the Center for Molecular Studies in Digestive and Liver Diseases). Behavior procedures were performed with The Neurobehavior Testing Core at University of Pennsylvania/Institute for Translational Medicine and Therapeutics and the Intellectual and Developmental Disabilities Research Center at Children's Hospital of Pennsylvania/University of Pennsylvania (National Institute of Child Health and Human Development Grant U54 HD086984). We thank J.A. Youssefian for material and logistical support. This work was supported by NIH grants RO1AA027202 (S.L.B.), T32 GM-07229 (D.C.A.), F31 CA247348-02 (M.M.), AARF-19-618159 (G.E.), K99AA027839 (P.M.), and K99AA028577 (G.E.).

Author affiliations: ^aEpigenetics Institute, University of Pennsylvania, Philadelphia, PA 19104; ^bDepartment of Genetics, University of Pennsylvania, Philadelphia, PA 19104; ^cDepartment of Biochemistry and Biophysics, Perelman School of Medicine, University of Pennsylvania, Philadelphia, PA 19104; ^dDepartment of Chemistry, University of Pennsylvania, Philadelphia, PA 19104; ^eDepartment of Clinical Biochemistry and Pharmacology, Faculty of Health Sciences, Ben Gurion University of the Negev, Beer-Sheva, 8410501, Israel; ^fDepartment of Neurobiology and Behavior, Center for the Neurobiology of Learning and Memory, University of California, Irvine, CA 92697; ^gEpivario, Inc., Philadelphia, PA 19104; ^hBeer-Sheva Mental Health Center, Ministry of Health, Anxiety and Stress Research Unit, Faculty of Health Sciences, Ben Gurion University of the Negev, Beer-Sheva, 8410501, Israel; ⁱFishberg Department of Neuroscience and Friedman Brain Institute, Icahn School of Medicine at Mount Sinai, New York, NY 10029; ^jDepartment of Cell and Developmental Biology, Perelman School of Medicine, University of Pennsylvania, Philadelphia, PA 19104; and ^kDepartment of Biology, University of Pennsylvania, Philadelphia, PA 19104

Author contributions: D.C.A., T.C., M.M., P.M., G.E., and S.L.B. designed research; D.C.A., T.C., M.M., A.G., T.B., R.W., R.R.C., J.H., A.A.K., J.W., M.A.W., and H.C. performed research; A.G., T.K., B.A.G., and H.C. contributed new reagents/analytic tools; D.C.A., T.C., and M.M. analyzed data; and D.C.A. and T.C. wrote the paper.

Reviewers: T.A., The University of Iowa; and E.V., Buck Institute for Research on Aging.

8. F. Petrij *et al.*, Rubinstein-Taybi syndrome caused by mutations in the transcriptional co-activator CBP. *Nature* **376**, 348–351 (1995).
9. J. H. Roelfsema *et al.*, Genetic heterogeneity in Rubinstein-Taybi syndrome: Mutations in both the CBP and EP300 genes cause disease. *Am. J. Hum. Genet.* **76**, 572–580 (2005).
10. F. Pietrocola, L. Galluzzi, J. M. Bravo-San Pedro, F. Madeo, G. Kroemer, Acetyl coenzyme A: A central metabolite and second messenger. *Cell Metab.* **21**, 805–821 (2015).
11. X. Li, G. Egervari, Y. Wang, S. L. Berger, Z. Lu, Regulation of chromatin and gene expression by metabolic enzymes and metabolites. *Nat. Rev. Mol. Cell Biol.* **19**, 563–578 (2018).
12. G. Egervari, K. M. Glasad, S. L. Berger, Food for thought. *Science* **370**, 660–662 (2020).
13. K. E. Wellen *et al.*, ATP-citrate lyase links cellular metabolism to histone acetylation. *Science* **324**, 1076–1080 (2009).
14. X. Li *et al.*, Nucleus-translocated ACSS2 promotes gene transcription for lysosomal biogenesis and autophagy. *Mol. Cell* **66**, 684–697.e9 (2017).
15. M. Mendoza *et al.*, Enzymatic transfer of acetate on histones from lysine reservoir sites to lysine activating sites. *Sci. Adv.* **8**, eabj5688 (2022).

16. P. Mews *et al.*, Acetyl-CoA synthetase regulates histone acetylation and hippocampal memory. *Nature* **546**, 381–386 (2017).
17. P. Mews *et al.*, Alcohol metabolism contributes to brain histone acetylation. *Nature* **574**, 717–721 (2019).
18. M. Xu *et al.*, An acetate switch regulates stress erythropoiesis. *Nat. Med.* **20**, 1018–1026 (2014).
19. S. A. Comerford *et al.*, Acetate dependence of tumors. *Cell* **159**, 1591–1602 (2014).
20. S. Lykke-Andersen, T. H. Jensen, Nonsense-mediated mRNA decay: An intricate machinery that shapes transcriptomes. *Nat. Rev. Mol. Cell Biol.* **16**, 665–677 (2015).
21. R. Nagaraj *et al.*, Nuclear localization of mitochondrial TCA cycle enzymes as a critical step in mammalian zygotic genome activation. *Cell* **168**, 210–223.e11 (2017).
22. G. Sutendra *et al.*, A nuclear pyruvate dehydrogenase complex is important for the generation of acetyl-CoA and histone acetylation. *Cell* **158**, 84–97 (2014).
23. M. Sarter, G. Bodewitz, D. N. Stephens, Attenuation of scopolamine-induced impairment of spontaneous alteration behaviour by antagonist but not inverse agonist and agonist β -carbolines. *Psychopharmacology (Berl.)* **94**, 491–495 (1988).
24. P. Curzon, N. R. Rustay, K. E. Browman, *Cued and Contextual Fear Conditioning for Rodents* (CRC Press/Taylor & Francis, 2009).
25. P. W. Frankland *et al.*, Stability of recent and remote contextual fear memory. *Learn. Mem.* **13**, 451–457 (2006).
26. C. S. Park, H. Rehrauer, I. M. Mansuy, Genome-wide analysis of H4K5 acetylation associated with fear memory in mice. *BMC Genomics* **14**, 539 (2013).
27. S. C. McQuown *et al.*, HDAC3 is a critical negative regulator of long-term memory formation. *J. Neurosci.* **31**, 764–774 (2011).
28. E. Palomer *et al.*, Aging triggers a repressive chromatin state at Bdnf promoters in hippocampal neurons. *Cell Rep.* **16**, 2889–2900 (2016).
29. S. Sidoli, N. V. Bhanu, K. R. Karch, X. Wang, B. A. Garcia, Complete workflow for analysis of histone post-translational modifications using bottom-up mass spectrometry: From histone extraction to data analysis. *J. Vis. Exp.* **2016**, 54112 (2016).
30. R. M. Barrett *et al.*, Hippocampal focal knockout of CBP affects specific histone modifications, long-term potentiation, and long-term memory. *Neuropsychopharmacology* **36**, 1545–1556 (2011).
31. T. Kutsuwada *et al.*, Impairment of suckling response, trigeminal neuronal pattern formation, and hippocampal LTD in NMDA receptor epsilon 2 subunit mutant mice. *Neuron* **16**, 333–344 (1996).
32. Y. P. Tang *et al.*, Genetic enhancement of learning and memory in mice. *Nature* **401**, 63–69 (1999).
33. A. Fischer, F. Sananbenesi, P. T. Pang, B. Lu, L. H. Tsai, Opposing roles of transient and prolonged expression of p25 in synaptic plasticity and hippocampus-dependent memory. *Neuron* **48**, 825–838 (2005).
34. F. Freudenberg, A. Alltoa, A. Reif, Neuronal nitric oxide synthase (*NOS1*) and its adaptor, *NOS1AP*, as a genetic risk factors for psychiatric disorders. *Genes Brain Behav.* **14**, 46–63 (2015).
35. M. A. Wood *et al.*, Transgenic mice expressing a truncated form of CREB-binding protein (CBP) exhibit deficits in hippocampal synaptic plasticity and memory storage. *Learn. Mem.* **12**, 111–119 (2005).
36. A. M. M. Oliveira, M. A. Wood, C. B. McDonough, T. Abel, Transgenic mice expressing an inhibitory truncated form of p300 exhibit long-term memory deficits. *Learn. Mem.* **14**, 564–572 (2007).
37. S. Peleg *et al.*, Altered histone acetylation is associated with age-dependent memory impairment in mice. *Science* **328**, 753–756 (2010).
38. H. Cohen, J. Zohar, M. Matar, The relevance of differential response to trauma in an animal model of posttraumatic stress disorder. *Biol. Psychiatry* **53**, 463–473 (2003).
39. J. Zohar, R. Sonnino, A. Juven-Wetzler, H. Cohen, Can posttraumatic stress disorder be prevented? *CNS Spectr.* **14**(1, suppl. 1), 44–51 (2009).
40. H. Pajouhesh, G. R. Lenz, Medicinal chemical properties of successful central nervous system drugs. *NeuroRx* **2**, 541–553 (2005).
41. Q. Chen *et al.*, 2,3-Substituted quinoxalin-6-amine analogs as antiproliferatives: A structure-activity relationship study. *Bioorg. Med. Chem. Lett.* **21**, 1929–1932 (2011).
42. J. L. Kwapis, M. A. Wood, Epigenetic mechanisms in fear conditioning: Implications for treating post-traumatic stress disorder. *Trends Neurosci.* **37**, 706–720 (2014).
43. R. M. Stilling *et al.*, K-lysine acetyltransferase 2a regulates a hippocampal gene expression network linked to memory formation. *EMBO J.* **33**, 1912–1927 (2014).
44. W. Wei *et al.*, p300/CBP-associated factor selectively regulates the extinction of conditioned fear. *J. Neurosci.* **32**, 11930–11941 (2012).
45. J. S. Guan *et al.*, HDAC2 negatively regulates memory formation and synaptic plasticity. *Nature* **459**, 55–60 (2009).
46. J. Gao *et al.*, A novel pathway regulates memory and plasticity via SIRT1 and miR-134. *Nature* **466**, 1105–1109 (2010).
47. L. Peixoto, T. Abel, The role of histone acetylation in memory formation and cognitive impairments. *Neuropsychopharmacology* **38**, 62–76 (2013).
48. L. F. Chen *et al.*, Enhancer histone acetylation modulates transcriptional bursting dynamics of neuronal activity-inducible genes. *Cell Rep.* **26**, 1174–1188.e5 (2019).
49. M. D. Carpenter *et al.*, Nr4a1 suppresses cocaine-induced behavior via epigenetic regulation of homeostatic target genes. *Nat. Commun.* **11**, 504 (2020).
50. C. G. Vecsey *et al.*, Histone deacetylase inhibitors enhance memory and synaptic plasticity via CREB:CBP-dependent transcriptional activation. *J. Neurosci.* **27**, 6128–6140 (2007).
51. A. Fischer, F. Sananbenesi, X. Wang, M. Dobbin, L. H. Tsai, Recovery of learning and memory is associated with chromatin remodelling. *Nature* **447**, 178–182 (2007).
52. S. Gupta *et al.*, Histone methylation regulates memory formation. *J. Neurosci.* **30**, 3589–3599 (2010).
53. A. L. Kung *et al.*, Gene dose-dependent control of hematopoiesis and hematologic tumor suppression by CBP. *Genes Dev.* **14**, 272–277 (2000).
54. T. P. Yao *et al.*, Gene dosage-dependent embryonic development and proliferation defects in mice lacking the transcriptional integrator p300. *Cell* **93**, 361–372 (1998).
55. M. A. Wood, M. A. Attner, A. M. M. Oliveira, P. K. Brindle, T. Abel, A transcription factor-binding domain of the coactivator CBP is essential for long-term memory and the expression of specific target genes. *Learn. Mem.* **13**, 609–617 (2006).
56. S. Chatterjee *et al.*, Pharmacological activation of Nr4a rescues age-associated memory decline. *Neurobiol. Aging* **85**, 140–144 (2020).
57. A. Nott *et al.*, Histone deacetylase 3 associates with MeCP2 to regulate FOXO and social behavior. *Nat. Neurosci.* **19**, 1497–1505 (2016).
58. Q. Jin *et al.*, Distinct roles of GCN5/PCAF-mediated H3K9ac and CBP/p300-mediated H3K18/27ac in nuclear receptor transactivation. *EMBO J.* **30**, 249–262 (2011).
59. R. L. Schiltz *et al.*, Overlapping but distinct patterns of histone acetylation by the human coactivators p300 and PCAF within nucleosomal substrates. *J. Biol. Chem.* **274**, 1189–1192 (1999).
60. J. Yu, I. de Belle, H. Liang, E. D. Adamson, Coactivating factors p300 and CBP are transcriptionally crossregulated by Egr1 in prostate cells, leading to divergent responses. *Mol. Cell* **15**, 83–94 (2004).
61. H. Takahashi, J. M. McCaffery, R. A. Irizarry, J. D. Boeke, Nucleocytosolic acetyl-coenzyme a synthetase is required for histone acetylation and global transcription. *Mol. Cell* **23**, 207–217 (2006).
62. J. J. Harris, R. Joliviet, D. Attwell, Synaptic energy use and supply. *Neuron* **75**, 762–777 (2012).
63. L. Cai, B. M. Sutter, B. Li, B. P. Tu, Acetyl-CoA induces cell growth and proliferation by promoting the acetylation of histones at growth genes. *Mol. Cell* **42**, 426–437 (2011).
64. T. J. Jarome, F. D. Lubin, Epigenetic mechanisms of memory formation and reconsolidation. *Neurobiol. Learn. Mem.* **115**, 116–127 (2014).
65. K. Nader, G. E. Schafe, J. E. LeDoux, Fear memories require protein synthesis in the amygdala for reconsolidation after retrieval. *Nature* **406**, 722–726 (2000).
66. S. Duvarci, K. Nader, J. E. LeDoux, De novo mRNA synthesis is required for both consolidation and reconsolidation of fear memories in the amygdala. *Learn. Mem.* **15**, 747–755 (2008).
67. J. Gräff *et al.*, Epigenetic priming of memory updating during reconsolidation to attenuate remote fear memories. *Cell* **156**, 261–276 (2014).
68. H. Yang, H. Wang, R. Jaenisch, Generating genetically modified mice using CRISPR/Cas-mediated genome engineering. *Nat. Protoc.* **9**, 1956–1968 (2014).
69. J. P. Concordet, M. Haeussler, CRISPOR: Intuitive guide selection for CRISPR/Cas9 genome editing experiments and screens. *Nucleic Acids Res.* **46** (W1), W242–W245 (2018).
70. D. Alexander, Targeting acetyl-CoA metabolism attenuates the formation of fear memories through reduced activity-dependent histone acetylation. NCBI Gene Expression Omnibus. <https://www.ncbi.nlm.nih.gov/geo/query/acc.cgi?acc=GSE199887>. Deposited 31 March 2022.
71. M. Mendoza, Targeting acetyl-CoA metabolism attenuates the formation of fear memories through reduced activity-dependent histone acetylation. Chorus. <https://chorusproject.org/pages/dashboard.html#projects/all/1745/experiments>. Deposited 10 February 2022.